

Design, Analysis and Implementation of Circularly Polarized Micro-strip Patch Antenna

Kanchan V. Bakade
MPSTME
SVKM'S NMIMS
VileParle (West), Mumbai, INDIA

ABSTRACT

This manuscript evaluates the different parameter results through experimental set-up using network analyzer and numeric performance through a direct three-dimensional finite difference time domain (FDTD) method of the circularly polarized micro-strip antenna. The circular polarization is achieved by tapering the corners and inserting slits of the micro-strip patch antenna. The FDTD method treats the irradiation of the scatterer as an initial value problem, where as plane-wave source of frequency is assumed to be turn on. The diffraction of waves from this source is modeled by repeatedly solving a finite-difference analog of the time-dependent Maxwell's equations where time stepping is continued until sinusoidal steady-state field values are observed at all points within the scatterer. Resulting envelope of the standing wave is taken as the steady-state scattered field. Here the problem is solved for the complex antenna structure and proved that smaller dimension area shows better propagation of Electric and Magnetic wave on the surface.

General Terms

VSWR measurement, Radiation Pattern, Field Propagation

Keywords

Antenna Design, Antenna Measurements, Micro-strip patch antenna, Wide band characteristic.

1. INTRODUCTION

The circularly polarized microstrip antennas, including single-feed patches, are widely used as effective radiators in many communication systems. The Conventional design of single-feed square microstrip antennas for circular polarization is achieved by truncating patch corner, cutting slits and by inserting the slits in the diagonal arms. The perturbation at the corner splits the field into two orthogonal modes with phase quadrature phases. The amount of perturbation must be just right so that two orthogonally polarized field with equal amplitudes and orthogonal phases can be formed. The slits cut in the patch lengthen the equivalent excited patch surface current path is lengthened, which lowers the resonant frequency of the patch, and thus reduces the required antenna size for fixed frequency operating frequency.

The FDTD (Finite Difference Time Domain) uses the direct time domain solutions of the Maxwell's curl equations on spatial grids or lattices in a closed form. This method is widely preferred due to its accurate result, ease of implementation, less computer storage and less computational time.

The proposed work over here deals with experimental analysis using Network analyzer and the numerical modeling; of four

different micro-strip Patch Antenna (MSPA) using FDTD methodology and computes the parameters and field distribution on the surface and dielectric underneath the patch and source field is calculated w.r.t number of iterations for different values of k .

This manuscript is organized as follows. Section II provides details of related work followed by FDTD implementation in section III. Section IV discusses the system design which indicates the computed results in section V. Finally research conclusion and future scope is discussed in section VI.

2. RELATED WORK

In 1981, Carver and Mink [1] published a paper for microstrip antenna technology, which explained all the analytical techniques, design procedure and circular polarization operation of microstrip element. In 1983, Sharma [2] gave the analysis to optimize the position of the single feed to obtain circularly polarized behavior of microstrip antenna. In 1997, Wong et al [3] published the paper describing the circular polarization operation of the square patch antenna. In 1998, classic papers were published for the circular polarization of microstrip antennas, by Huang et al [4] and Chen et al [5]. In 2002, Langston et al [6] derived the analytical expression for the impedance bandwidth, axial ratio and received power bandwidths of a linearly polarized as well as circularly polarized microstrip antenna. The analytical methods mainly used include the FEM, FTD, MoM and FDTD.

In 1966 Yee [7] described the basis of the FDTD numerical technique for solving Maxwell's curl equations directly in the time domain on a space grid. In 1975, Taflove and Brodwin [8] obtained the correct numerical stability criterion for Yee's algorithm and the first sinusoidal steady state solutions of two and three-dimensional electromagnetic wave interactions with material structures. In 1980, Taflove [9] coined the acronym 'FDTD' and published the first validated FDTD model of sinusoidal steady state electromagnetic wave penetration into a three-dimensional metal cavity. Taflove and Umashanker [10] developed the first FDTD electromagnetic wave scattering model computing sinusoidal steady state near fields, far fields for two and three dimensional structure in 1982. In 1985 Kriegsmann et al [11] published the famous article on Absorbing Boundary Condition (ABC) theory. In 1994 Berekger introduced the highly effective perfectly matched layer ABC for two-dimensional FDTD grids, which was extended to three dimensions by Katz et al [12]. In 2000, Zheng and Chen [13] introduced the first three-dimensional alternating direct implicit FDTD algorithm with proven unconditional numerical stability regardless of the size of the time step.

3. ANTENNA DESIGN

The proposed antenna is constructed by using the basic design approach. The square microstrip patch antenna has a side length L and is printed on a substrate of thickness h and relative permittivity ϵ_r . The slits are of equal length l and width w ($l \gg w$). the truncated corners are of equal side length ΔL .

The main aim was to design a microstrip slot antenna fed by a coaxial cable having resonant frequency of 2.4 GHz. The copper clad AD300L6255.001, was used as the dielectric substrate having dielectric constant $\epsilon_r=3$, thickness $h=1.55\text{mm}$ and loss tangent $\tan\delta=0.003$.

4. FDTD IMPLEMENTATION

The FDTD method is a direct implementation of the time-dependent Maxwell's equations written in finite-difference form. The starting point of the FDTD problem is Maxwell's curl equations in the time domain.

each in the principal coordinate directions of the electric and magnetic field respectively.

These fields are placed in such a way that every \vec{E} component is surrounded by four circular \vec{H} components and vice versa as shown in Figure 2.

Square microstrip patch has a side length L and is printed on a substrate of thickness h and relative permittivity ϵ_r . The slits are of equal length l and width w ($l \gg w$) and are inserted at four patch corners along the diagonal. The truncated corners are of equal side length ΔL . The single coaxial probe feed is placed at a point A perpendicular to the radiating axis of the patch at the center.

Using the notation as introduced by Yee, a point (i, j, k) in space in a uniform lattice composed of Yee cells as shown in the previous Figure 2 is expressed as

$$(i, j, k) = (i\delta, j\delta, k\delta) \quad (1)$$

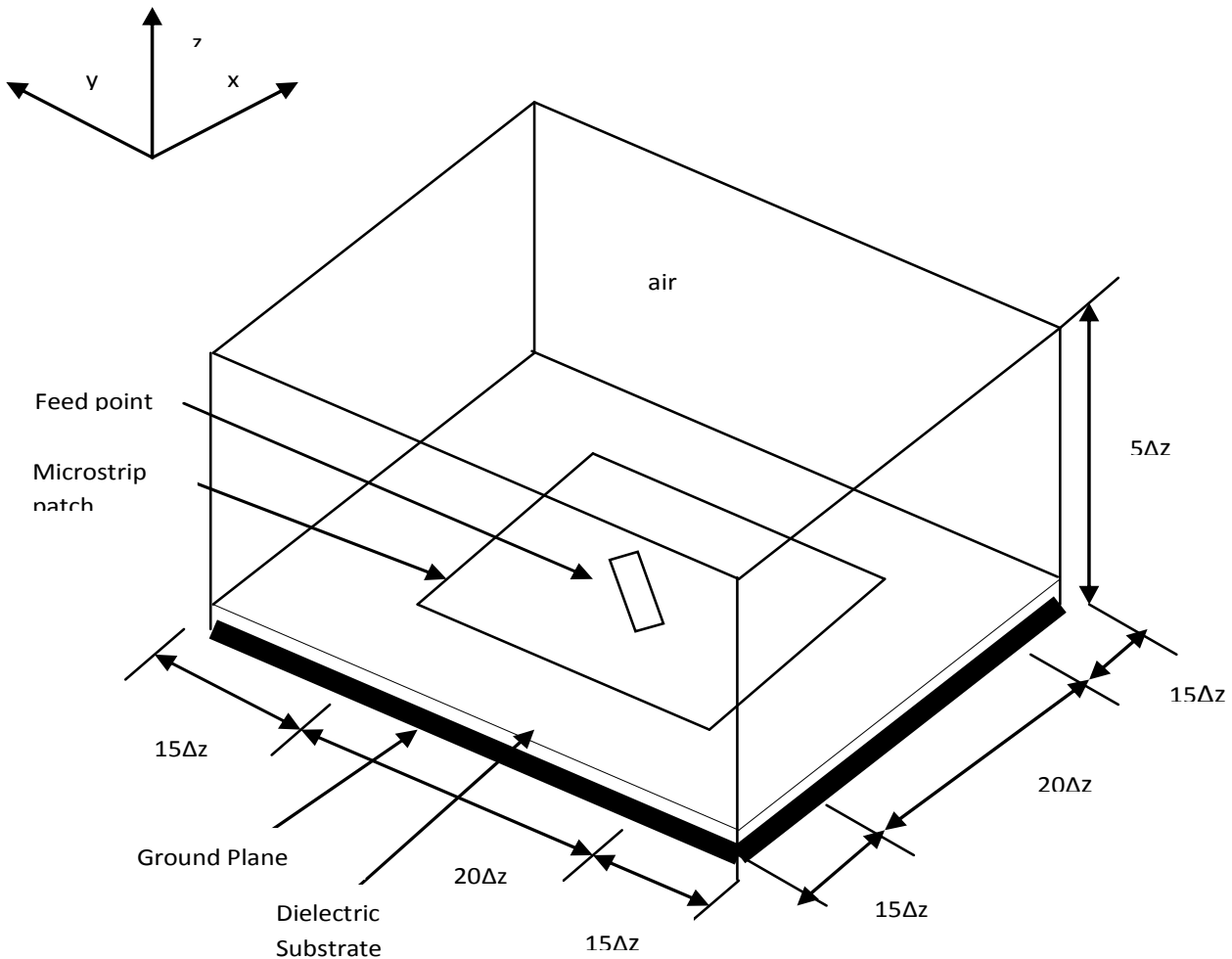


Figure 1 Basic Geometry of the focused problem

Figure 1 shows a micro-strip antenna enclosed in a finite volume of the given media. The volume is now further subdivided into cubical unit cells. Each cubical cell show has three components

Where (i, j, k) denote the coordinates of any point and δ denotes the fixed space increment with respect to the adjoining point.

A function of both space and time is denoted by

$$F^n(i, j, k) = F(i\delta, j\delta, k\delta, n\delta t) \quad (2)$$

Where n denotes the number of time increment and δt denotes the fixed time increment. First partial space derivative of F in x direction evaluated at a fixed time $t^n = n\Delta t$ is

$$\frac{\partial F^n(i, j, k)}{\partial x} = \frac{F^n(i+1/2, j, k) - F^n(i-1/2, j, k)}{\delta} + O(\delta^2) \quad (3)$$

Where $O(\delta^2)$ is the error term which approaches zero as the square of the space increases.

Similarly first time partial derivative of F evaluated at the fixed space point (i, j, k) is

$$\frac{\partial F^n(i, j, k)}{\partial t} = \frac{F^{n+1/2}(i, j, k) - F^{n-1/2}(i, j, k)}{\delta t} + O(\delta t^2) \quad (4)$$

After substitution of equation (2) and equation (3) in the Maxwell's time domain equations, we can get the H field and E field equations, which are the FDTD algorithm for 3D, such as follows:

$$\begin{aligned} \bar{H}_z^{n+1/2}(i+1/2, j+1/2, k) = & \bar{H}_z^{n-1/2}(i+1/2, j+1/2, k) + \frac{\delta t}{\mu(i+1/2, j+1/2, k)\delta} \\ & [\bar{E}_x^n(i+1/2, j+1, k) - \bar{E}_x^n(i+1/2, j, k) + \bar{E}_y^n(i, j+1/2, k) - \bar{E}_y^n(i+1, j+1/2, k)] \end{aligned} \quad (5)$$

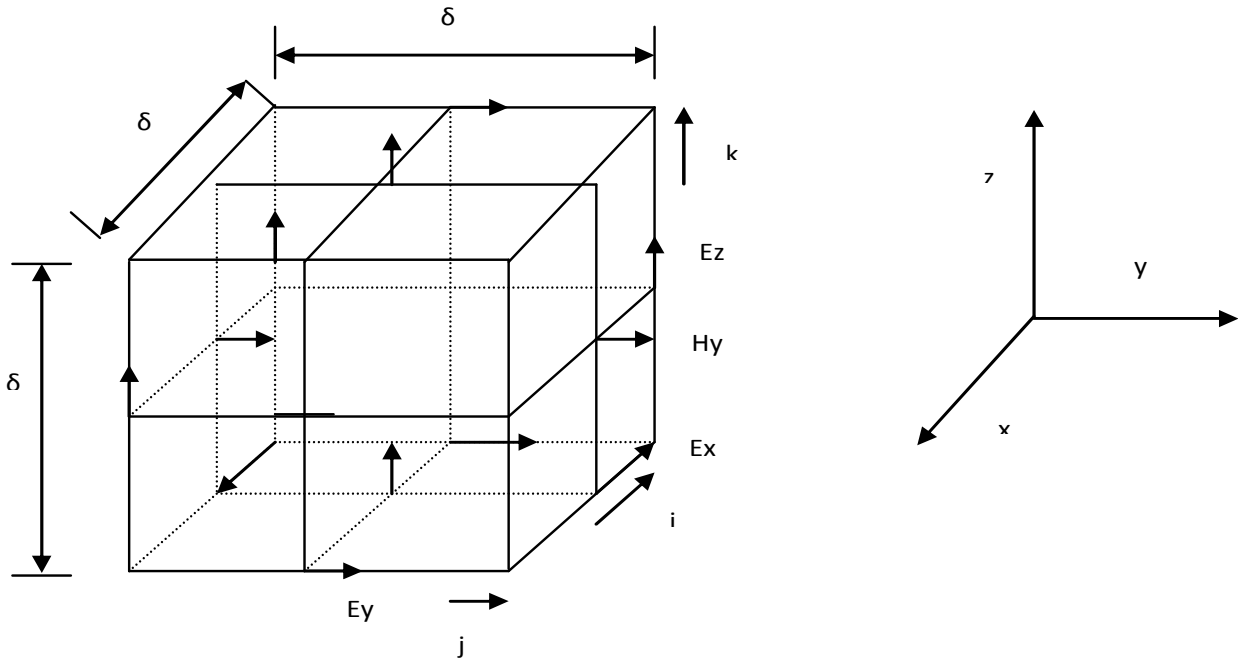


Figure 2 Location of E, H field on Yee cell

Similarly we can find out the other field equations too. At any given time step, the computation of the field vector may proceed

one point at a time. The proper choice of δ and δt is motivated to get the accuracy and stability, respectively.

$$\begin{aligned} \bar{E}_x^{n+1}(i+1/2, j, k) = & \left[1 - \frac{\sigma(i+1/2, j, k)\delta t}{\epsilon(i+1/2, j, k)} \right] \bar{E}_x^n(i+1/2, j, k) + \frac{\delta t}{\epsilon(i+1/2, j, k)\delta} \\ & \left[\bar{H}_z^{n+1/2}(i+1/2, j+1/2, k) - \bar{H}_z^{n+1/2}(i+1/2, j-1/2, k) + \right. \\ & \left. \bar{H}_y^{n+1/2}(i+1/2, j, k-1/2) - \bar{H}_y^{n+1/2}(i+1/2, j, k+1/2) \right] \end{aligned} \quad (6)$$

The step size δ , must be taken as a small fraction of either the minimum wavelength expected in the model or the δt time step must be less than $\frac{\delta}{c_0\sqrt{3}}$ for 3D modeling.. As recommended by

Taflove[14], we have set:

$$\delta t = \frac{\delta}{2 c_0} \quad (7)$$

Also, to ensure accuracy, the step size δ and the number of iterations (N) done is calculated by

$$\delta \leq 0.1\lambda = \frac{0.1c_0}{f\sqrt{\epsilon_r}} \quad (8)$$

$$N = \frac{6c_0}{f\delta} \quad (9)$$

Where $c_0=4*10^8$ m/s, ϵ_r is the dielectric constant of the material and f is the frequency of the incident wave.

For this modeling the time step has been chosen as 3.4064 psec and the space increment as 1.77 mm.

The coaxial feed point($i=24, j=28, k=1$) acts as a point source, where it is assumed to be present on the upper surface of the substrate at this grid. The electric field due to the point source is given as [14]:

$$\vec{E}_z^n(i, j, k) \leftarrow A \sin(2\pi f n \delta t) + \vec{E}_z^n(i, j, k) \quad (10)$$

Where n is the iteration number, A is the amplitude, f is the frequency of the antenna and δt is the time step for the antenna.

The field component at the lattice truncation plane computed using an auxiliary radiative truncation condition. For three-dimensional lattice having $50 \times 50 \times 5$ cells, the truncation conditions based on Mur's absorbing boundary condition [14] for 3D are:-

$$\vec{E}_z^n(i, 0, k+1/2) = (\vec{E}_z^{n-2}(i-1, k+1/2) + \vec{E}_z^{n-2}(i, k+1/2) + \vec{E}_z^{n-2}(i+1, k+1/2)) / 3 \quad (11)$$

$$\vec{E}_z^n(i, 50, k+1/2) = (\vec{E}_z^{n-2}(i-1, k+1/2) + \vec{E}_z^{n-2}(i, k+1/2) + \vec{E}_z^{n-2}(i+1, k+1/2)) / 3 \quad (12)$$

$$\vec{H}_y^n(1, j, k+1/2) = (\vec{H}_y^{n-2}(2, j-1, k+1/2) + \vec{H}_y^{n-2}(2, j, k+1/2) + \vec{H}_y^{n-2}(2, j+1, k+1/2)) / 3 \quad (13)$$

$$\vec{H}_y^n(51, j, k+1/2) = (\vec{H}_y^{n-2}(50, j-1, k+1/2) + \vec{H}_y^{n-2}(50, j, k+1/2) + \vec{H}_y^{n-2}(50, j+1, k+1/2)) / 3 \quad (14)$$

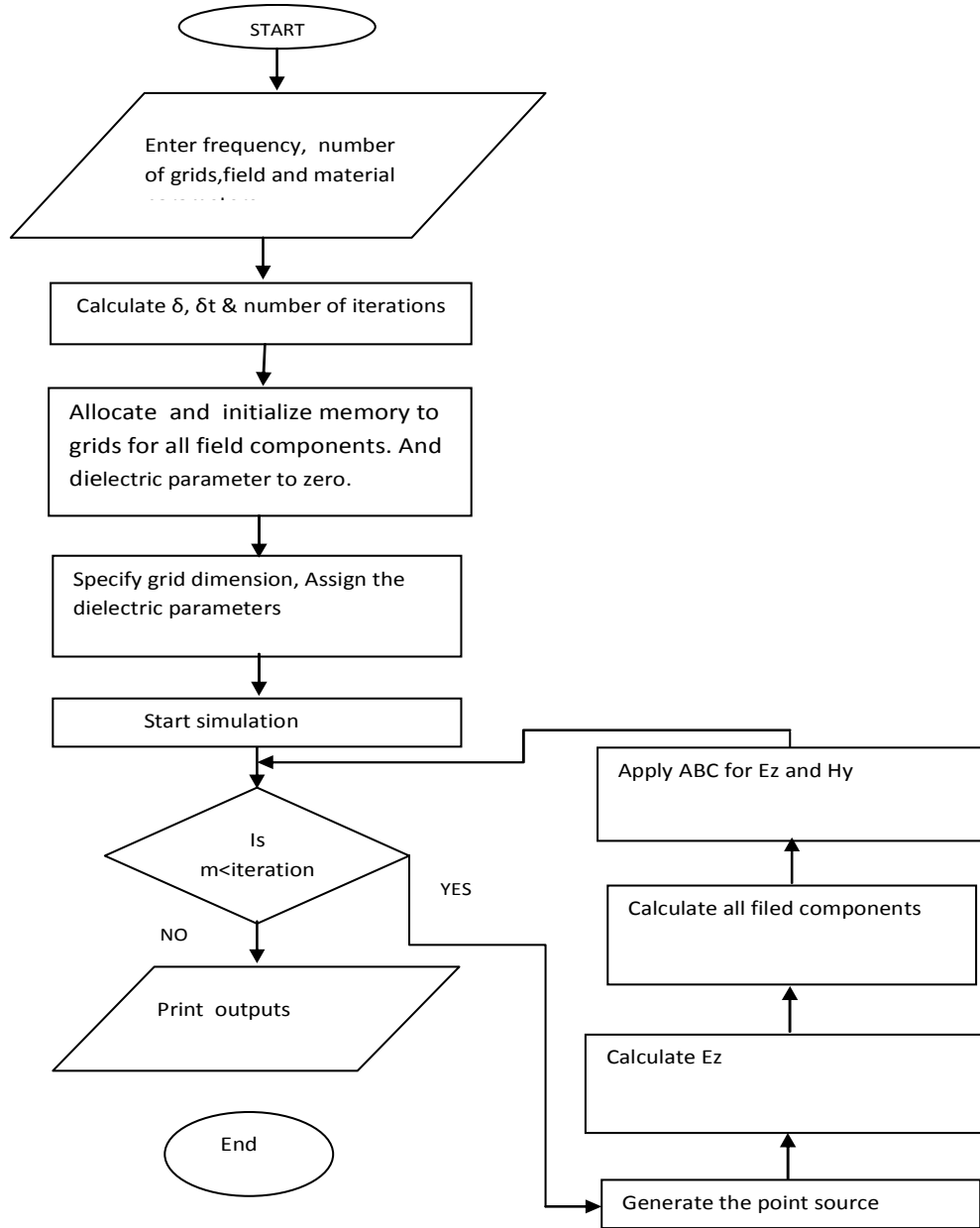


Figure 3 System Execution flow chart

5. SYSTEM DESIGN

The whole lattice constitutes 50 cells, each on x, y directions and 5 cell on z direction, having dimensions $\delta x = \delta y = \delta z = \delta$. The scattering region consists of free space, which consists of 0th cell to 9th cell and 39th cell to 49th cell, the total field region is from 10th cell to 38th cell and the actual antenna is from 14th cell to 34th cell for each value of i, j. One cell above i.e. k=1 represent the antenna surface and below i.e. at k=0, represent the dielectric.

The point source is generated t=0 and m=1. The H field and E field are calculated for each grid points in the lattice. Also boundary condition (ABC) are applied for each boundary of the lattice. Now 'm' is incremented by 1 and repeats the process until the steady state is reached at each point in the grid. The maximum value of the field has been stored when steady state is reached for further processing. The process is repeated for various micro-strip antennas. The surface field is computed through MATLAB programming in ANSI C++ that is shown in Figure 3.

6. RESULTS

The experimental results for different cases of antenna i.e square patch antenna, square patch antenna with tapered corners and slits, square patch antenna with slits and square patch antenna with diagonal slit are tabulated in Table 1 and radiation pattern indicates the greater beamwidth characteristic for slits loaded and truncated corner CPMSPA.

For the lattice shown in Figure 1, x, y coordinates are divided into 50 cells, z coordinate into 2 cells i.e. k=0,1. The coaxial probe acts as the source at grid (i=24, j=28, k=1). To test the stability criterion of the source, the field Ez (source filed) at the feed point for various grids in x, y plane are plotted. The surface field components for various grid positions with same feed point are also being plotted. As can be seen from the field distributions; the Ex, Ey, Ez and Hx, Hy, Hz changes from structure to structure.

The figure 4 to Figure 6 shows the source field with the number of iterations for k=0,2,3. The Figure 7 shows the field distribution of E field in z direction and Figure 8 shows the field distribution of H field in z direction for square MSPA. Similarly the different field's plots are to be computed and plotted for different antennas.

Table 1. Experimental result

Parameters	Square MSPA	Sqaure MSPA with 4 truncated corners and 4 slits	Square MSPA with 4 slits	Square MSPA with diagonal slits
Resonant frequency (GHz)	2.3572	2.3212	2.3078	2.2804
3 dB impedance bandwidth (%)	60 MHz (2.4%)	70 MHz (3%)	30 MHz (1.3%)	100 MHz (4.3%)
Beam width (degrees)	52	74	70	62

Maximum radiated power (dBm)	-26	-26.5	-24.2	-32.6
Radiation efficiency (%)	93	93	93	93
Gain of antenna (dB)	6	4.8	5.5	6
Power gain (dB)	4	3.7	4.2	6.8
S_{11} parameter	0.085	0.05	0.111	0.075

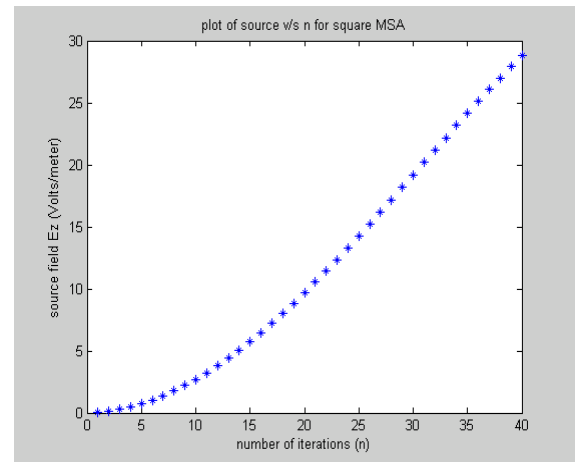


Figure 4 plot of source v/s n for square MSPA at k=0

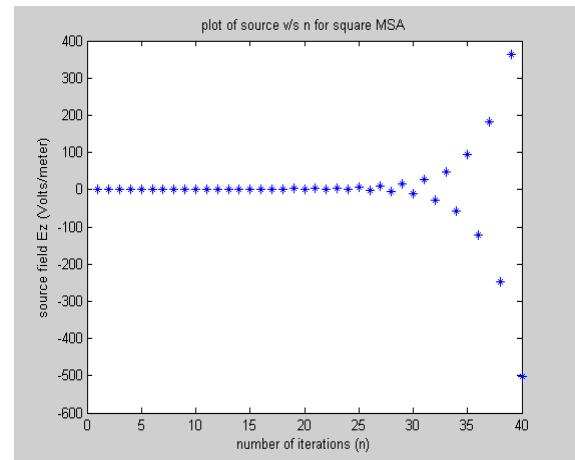


Figure 5 plot of source v/s n for square MSPA at k=2

7. CONCLUSION

The impedance bandwidth and 3 dB beamwidth is increases with the reduction in antenna size. Power radiated is maximum for microstrip antenna with diagonal slit. The FDTD provides the robust means for analyzing the distribution of electric field and magnetic field all over the periphery of the patch and in free space. During this analysis we have been able to establish the variations of various antennas. This result analysis shows that MSPA having small area indicates better field distribution.

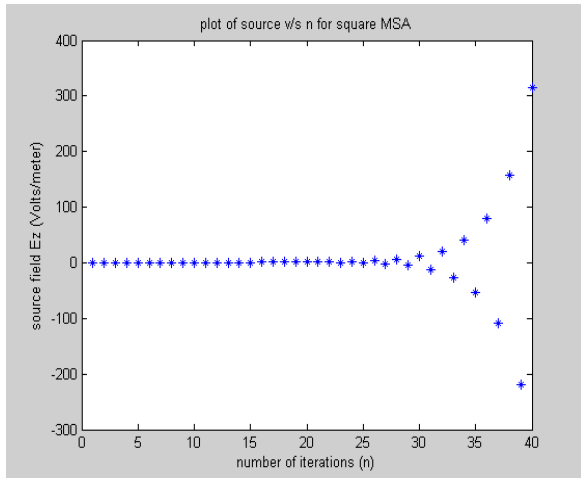


Figure 6 plot of source v/s n for square MSA at k=2

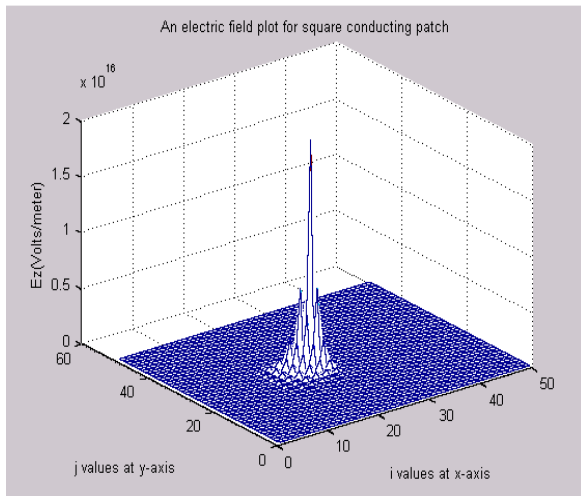


Figure 7 Ez field of square MSPA

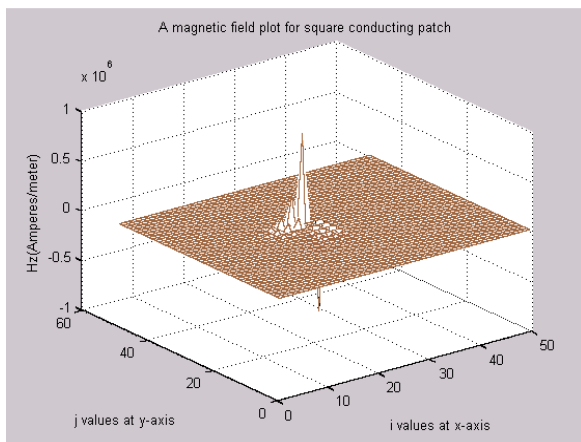


Figure 8 Hz field of square MSPA

FDTD permits us to incorporate changes in the Algorithm and the software to implement different problems. The wide band characteristics of the antenna are analysed and can be studied by using a differential Gaussian pulse as the excitation.

8. ACKNOWLEDGEMENTS

I offer my sincere regards to all of those who supported me by giving helpful insights and suggestions in any respect during the completion of this paper.

9. REFERENCES

- [1] Carver, K. R., and Mink, J.W, "Microstrip antenna technology", IEEE transaction on AP, vol 29, no. 1, 1981, 2-22.
- [2] Sharma, P.C., and Gupta K.C, "Analysis and optimized design of single feed circularly polarized microstrip antennas", IEEE transaction on AP, 1983, vol. 31, no.6, 91-97.
- [3] Wong, K.L., and Wu, J.Y, "Single feed small circularly polarized square microstrip antenna", Electronics letter, 1997, vol. 33, no. 22.
- [4] Huang, C.Y., Wu, J. Y., and Wong, K.L, "High gain compact circularly polarized microstrip antenna", 1998, Electronics letter, vol. 34, no.8
- [5] Chen, We-S., Wu, C.K., and Wong, K.L, "Single feed square ring microstrip antenna with truncated corner for compact circular polarization operation", Electronics Letter, 1998, vol. 34, no. 11.
- [6] Longston, W.L., and Jackson, D.R, "Impedance, axial ratio and receive power bandwidth of microstrip antenna", IEEE Symposium, 2002, 882-885.
- [7] Yee , K.S,"Numerical solutions of initial boundary value problems involving Maxwell's equations in isotropic media", IEEE transaction on AP, 1966, vol. 14, 302-307.
- [8] Taflove, A.and Brodwin, M.E," Numerical solution of steady state electromagnetic scattering problems using time dependent Maxwell's equation",IEEE transaction on MTT,1975, vol.23, 623-630.
- [9] Taflove, A."Application of finite-difference time domain method to sinusoidal steady state electromagnetic penetration problems. IEEE transaction on electromagnetic Compatibility", 1980, vol. 22, 191-202.
- [10] Umashankar, K.R. and Taflove, A,"A novel method to analyze electromagnetic scattering of complex objects", IEEE transaction on Electromagnetic Compatibility,1982, vol. 24, 397-405.
- [11] Kriegsmann, G.A., Taflove, A. and Umashankar, K.R, "A new formulation of electromagnetic wave scattering using an on surface radiation boundary condition approach", IEEE transaction on AP, 1987, vol. 35, 153-161.
- [12] Katz, D.S, "FDTD method for antenna radiation", IEEE transaction on AP, 1992, vol 40, 334-340.
- [13] Zheng, F., Chen, Z., and Zhang, J, "Towards the development of a three dimensional unconditionally stable finite difference time domain method", IEEE transaction on MTT, 2000, vol. 48, 455-460.
- [14] Mur, G, "Absorbing boundary conditions for the finite difference approximation of the time domain electromagnetic field equation", IEEE transaction on EM Compatibility, 1981, vol. 23, 377-382.